

Modelling post-frying oil absorption, water loss, and cooling of potato cylinders

¹Del Rosario-Santiago, J., ²López-Méndez, E. M., ¹Ruiz-Espinosa, H.,
³Ochoa-Velasco, C. E., ¹Escobedo-Morales, A. and ^{1*}Ruiz-López, I. I.

¹Facultad de Ingeniería Química, Benemérita Universidad Autónoma de Puebla,
 Av. San Claudio y 18 Sur. Ciudad Universitaria, C.P. 72570, Puebla, México

²Universidad Tecnológica de Izúcar de Matamoros,

Prolongación Reforma 168, C.P. 74420, Izúcar de Matamoros, Puebla, México

³Facultad de Ciencias Químicas, Benemérita Universidad Autónoma de Puebla,
 Av. San Claudio y 18 Sur. Ciudad Universitaria, C.P. 72570, Puebla, México

Article history

Received:

26 November 2021

Received in revised form:

9 November 2022

Accepted:

17 July 2023

Keywords

conduction,

cooling,

evaporation rate,

oil penetration

Abstract

A simultaneous heat and mass transfer model based on global coefficients was proposed to describe the oil absorption, water loss, and temperature changes occurring during the post-frying period of potato cylinders. The model was solved in Matlab® and simultaneously fitted to post-frying kinetics from literature, describing the surface and penetrated surface oil contents, as well as the surface and centre temperatures of potato cylinders at six holding temperatures (25, 100, 120, 140, 160, and 180°C). Besides, simple algorithms were developed to evaluate the oil layer thickness and the minimum oil penetration distance, obtained by assuming the potato cylinder was split into a dry zone, where the oil was absorbed, and a moist zone free from oil. The model achieved a good reproduction of fitted responses with average deviations ranging from 1.9 to 11.7% for all post-frying holding temperatures. Estimated distribution coefficients evidenced higher oil absorption at low holding temperatures, increasing from 0.66 kg surface oil/kg absorbed oil at 25°C to 2.60 kg surface oil/kg absorbed oil at 180°C, while no temperature influence on mass transfer coefficient was found under the explored experimental conditions ($p > 0.05$). The estimated minimum oil penetration distance (thickness of the dry zone region) after the post-frying stage (229 to 506 μm) showed a good agreement with crust thickness values from literature.

Nomenclature

c_s : solids concentration in potato (kg/m^3); C_p : specific heat ($\text{J}/\text{kg}/^\circ\text{C}$); d : minimum oil penetration distance (m); D : effective oil diffusivity (m^2/s); E : activation energy (J/mol); h : heat transfer coefficient ($\text{W}/\text{m}^2/^\circ\text{C}$); K : partition coefficient of oil (kg surface oil/kg absorbed oil); k_0 : parameter adjusting the evaporation rate ($\text{m}/\text{kPa}/\text{s}$); k_c : first-order rate constant ($1/\text{s}$); k_h : heat transfer coefficient ($\text{W}/\text{m}^2/^\circ\text{C}$); k_m : mass transfer coefficient (m/s); k_{m0} : preexponential factor (m/s); l : length of potato cylinders (m); m : mass (kg); MRD : mean relative deviation; N : mass flux (kg/s); O : surface oil content, dry basis (kg oil/kg solids); p : pressure (kPa); q : heat flux (W); R : radius of potato cylinders (m); \dot{R} : water loss rate ($\text{kg}/\text{m}^2/\text{s}$); R_g : universal gas constant ($\text{J}/\text{mol}/\text{K}$); S : surface (m^2); SSE : sum of squared errors; T : temperature ($^\circ\text{C}$); $T\theta$: absolute temperature (K); V : volume (m^3); x : mass fraction of a given component in dry fat-free solids (kg/kg); X : mass fraction (kg/kg); W : water content in potato, dry basis (kg water/kg solids); and Y : penetrated oil content, dry basis (kg oil/kg solids).

Greek symbols

δ : effective film thickness where the heat and mass transfer occur (m); Δ : characteristic length for conduction (m); ϕ : geometrical factor (dimensionless); κ : thermal conductivity ($\text{W}/\text{m}/^\circ\text{C}$); λ : latent heat of vaporisation of water (J/kg); λ_1 : first eigenvalue of the analytical solution for heat or mass transfer; ρ : density (kg/m^3); σ : specific surface ($1/\text{m}$); and ξ : length-to-diameter ratio of the potato cylinders.

Subscripts

0: denotes the initial state; α : denotes the oil layer-food interface; β : denotes the oil layer-air interface; a : for ashes; air : for air; c : for carbohydrates; $center$: denotes the centre of the potato cylinder; e : denotes the equilibrium state; exp : denotes an experimental result; f : for fibre; F : for potato (food); L : for oil layer; max : denotes a maximum value; $pred$: denotes a predicted result; o : for oil; p : for protein; s : for fat-free solids; sat : saturation; and w : for water.

DOI

<https://doi.org/10.47836/ifrj.30.5.05>

© All Rights Reserved

*Corresponding author.

Email: irving.ruiz@correo.buap.mx

Introduction

Deep-fat frying is a unit operation where foods are cooked by immersion in hot oil at temperatures above the boiling point of water, typically ranging from 150 to 220°C (Devi *et al.*, 2020; Gouyo *et al.*, 2021b). The food is not only partially dewatered, but it also absorbs oil while developing unique flavour, colour, and texture characteristics (Kumar *et al.*, 2017). When fried, foods develop an outer dry crust, while the core remains moist and soft (Devi *et al.*, 2020; Gouyo *et al.*, 2021a). Most of the oil gained by food remains confined to the surface region immediately after frying (Khalilian *et al.*, 2021; Al Faruq *et al.*, 2022). This oil gradually infiltrates the crust during the post-frying cooling period (Bouchon and Pyle, 2005a; Touffet *et al.*, 2020). As fried foods increase their oil content up to 40% in mass, this is a major concern for health-conscious consumers (He *et al.*, 2012; Wanakamol and Poonlarp, 2018; Topete-Betancourt *et al.*, 2020); thus, an adequate characterisation of this stage is paramount to develop strategies for minimising the post-frying oil absorption.

Methods for removing the adhered surface oil after frying are gaining interest from the food industry (Liberty *et al.*, 2019). For example, centrifugation has been demonstrated as an effective method for post-frying de-oiling (Kim and Moreira, 2013; Khalilian *et al.*, 2021). Post-frying microwave heating produces French fries with lower oil content and better features (Zhou *et al.*, 2022). Applied pressure (atmospheric and vacuum drainage) and temperature also show an important effect on post-frying oil absorption (Debnath *et al.*, 2009; Tarmizi and Niranjani, 2013a; 2013b; Sosa-Morales *et al.*, 2022). The cooling-phase effect after frying affects the final oil content of fried products; therefore, selected studies have highlighted the need for developing mathematical models to describe this stage (Bouchon and Pyle, 2005a; 2005b; He *et al.*, 2012; Dehghannya and Ngadi, 2021). In this sense, Bouchon and Pyle (2005a; 2005b) developed and tested a predictive model for post-frying cooling where oil absorption was considered a pressure-driven flow due to capillary forces. The cooling stage was formulated as an unsteady-state conduction process where the amount of evaporated water was assumed negligible. He *et al.* (2012) also investigated the temperature and pressure gradients during post-

frying at vacuum and atmospheric pressure. The mathematical models formulated by Bouchon and Pyle (2005a; 2005b) and He *et al.* (2012) allowed the prediction of a higher capillary oil suction at low holding temperatures. Neither of these studies performed surface and penetrated oil surface measurements to experimentally appraise the oil migration. To the best of the authors knowledge, this task has only been performed by Debnath *et al.* (2009). These authors also formulated a mass transfer model with equilibrated surface to evaluate the mass transfer rate and mass equilibrium. Unfortunately, the available literature on the modelling of post-frying cooling and oil absorption remains very limited, and several aspects remain unexplored such as the possible water loss and evaporative cooling effects.

Therefore, the present work was aimed at developing a simultaneous heat and mass transfer model to describe the surface oil absorption, water loss, and temperature history (oil layer, surface, centre, and averaged) during the post-frying of potato cylinders. The model was used to estimate heat and mass transfer parameters such as heat and mass transfer coefficients, evaporation rate, and mass partition coefficients. In addition, algorithms were proposed to determine the thickness of the initial surface oil layer and the minimum oil penetration distance.

Materials and methods

Model development

General assumptions

The proposed post-frying model described the heat and mass exchange occurring between the oil surface layer (L), the fried potato cylinder, also referred as food (F) in some instances for simplicity, and the surrounding air (air). A schematic diagram showing the involved phases and relevant dimensions of the investigated system are shown in Figure 1a, while the heat and mass transfer fluxes occurring during the post-frying cooling of potato cylinders are depicted in Figure 2. The fried potato sample was represented as a finite cylinder of radius (R) and length (l); however, the proposed model was not restricted to this geometry, and can be easily generalised to consider other product shapes. A subscript α denoted the oil layer (OL)-food boundary, while a subscript β was used for the OL-air interface.

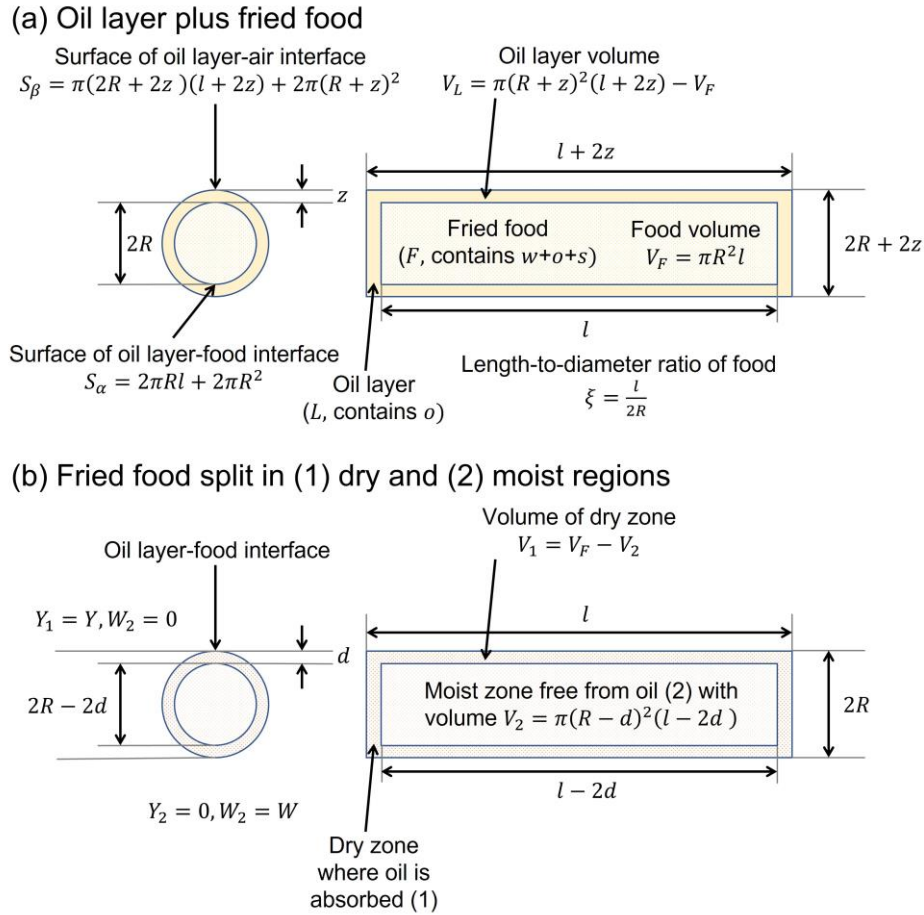


Figure 1. Dimensions of the explored system in (a) post-frying oil absorption model and (b) algorithm to evaluate the minimum distance for oil absorption. Refer to nomenclature section for a detailed description of all symbols.

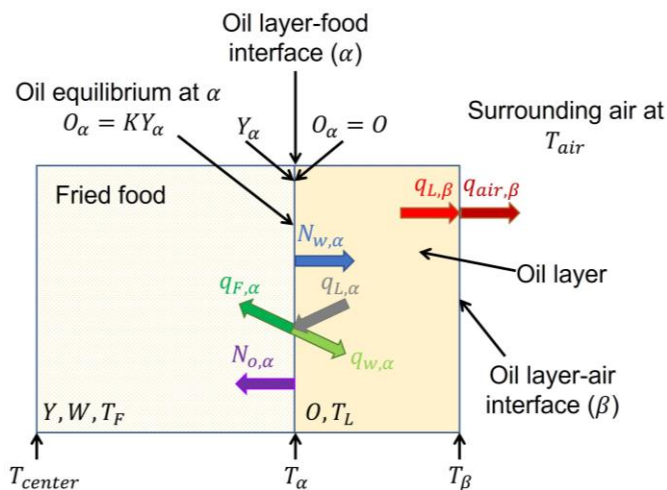


Figure 2. Schematic view of the investigated system showing relevant characteristics, and heat and mass fluxes in post-frying oil absorption model. Energy fluxes at α : $q_{L,\alpha} = k_{hL,\alpha}(T_\alpha - T_L)S_\alpha$ (oil side) and $q_{F,\alpha} = k_{hF,\alpha}(T_F - T_\alpha)S_\alpha$ (food side), energy fluxes at β : $q_{L,\beta} = k_{hL,\beta}(T_\beta - T_L)S_\beta$ (oil side) and $q_{air,\beta} = h(T_{air} - T_\beta)S_\beta$ (air side), flux of evaporated water at

α : $N_{w,\alpha} = -\dot{R}S_\alpha$ (this flux has the same form at both sides of the boundary), energy spent in water evaporation: $q_{w,\alpha} = \lambda N_{w,\alpha}$, oil flux at α (food side): $N_{o,\alpha} = k_m c_s (Y_\alpha - Y) S_\alpha$. Refer to nomenclature section for a detailed description of all symbols.

Mass balances were referred to the amounts of water (W), absorbed oil (Y), and surface oil (O), all expressed per mass of fat-free solids in potato samples, and considered to remain constant throughout the process. Several assumptions were made to simplify the model development as follows: (1) the potato cylinder consists of water (w), oil (o), and fat-free solids (s), and is covered after frying by an OL of uniform thickness (z); (2) the OL offers a negligible resistance to oil penetration into potato; (3) the OL remains free of any other component during post frying cooling; (4) the OL neither accumulates water nor offers a significant resistance to water loss; (5) the potato sample loses water as vapour during cooling; (6) heat transfer within both the OL and

potato specimen is controlled by a conduction mechanism; (7) heat transfer from OL to air is based on a convection mechanism; (8) the potato cylinder does not shrink during post-frying cooling; and (9) the mass of oil absorbed by the potato sample is equal to the mass loss of the OL. Apart from assumptions (4) and (5), all of them have been either explicitly or implicitly applied in other studies (Bouchon and Pyle, 2005a; Debnath *et al.*, 2009). Water loss of potato samples during post-frying cooling has been described in some studies (Tarmizi and Niranjani, 2013a), but its modelling has not been investigated yet. On the other hand, the OL is expected to provide a non-significant resistance to water loss due to both its low thickness (value of which was estimated in the present work), and the high pressure of water vapour caused by the food temperature.

Oil mass balances

The mass balance for penetrated surface oil (Y) in the potato cylinder was expressed in terms of a global mass transfer coefficient (k_m), using Eq. 1:

$$V_F c_s \frac{dY}{dt} = k_m c_s (Y_\alpha - Y) S_\alpha \quad (\text{Eq. 1})$$

where, V_F = volume of the potato cylinder, c_s = concentration of dry fat-free solids in potato (hereafter named solids for simplicity), Y = bulk oil content in potato sample (dry basis), Y_α = oil content (dry basis) at the OL-food boundary (food side), and S_α = contact surface between the food and the OL regions. Eq. 1 states that the accumulation rate of oil mass in potato cylinder ($V_F c_s dY/dt$) is equal to the mass flux of oil crossing the OL-food boundary ($N_{o,\alpha} = k_m c_s (Y_\alpha - Y) S_\alpha$). The non-penetrated surface oil content (O , dry basis) can be estimated from the mass balance as shown in Eq. 2:

$$O_{init} - O = Y - Y_{init} \quad (\text{Eq. 2})$$

where, $init$ = initial state. Eq. (2) establishes that the oil mass lost by the OL ($O_{init} - O$) equals that permeating the potato specimen ($Y - Y_{init}$). An average mass partition coefficient (K) is proposed to relate the oil concentrations at both sides of the OL-food interface as shown in Eq. 3:

$$O_\alpha = KY_\alpha \quad (\text{Eq. 3})$$

where, $O_\alpha = O$ because of the assumption of negligible OL resistance to mass transfer. Mass

balances such as that expressed in Eq. 1 and equilibrium partition models like Eq. 3 very often arise in the mathematical description of other mass transfer processes such as solid-gas adsorption, supercritical fluid extraction, and convective drying (Pakowski and Mujumdar, 2015; Promraksa *et al.*, 2020; Torres-Ramón *et al.*, 2021; Thorpe, 2022).

Water mass balance

The water in the potato cylinder was lost as vapour, but it did not accumulate in the OL, which remained water-free during post frying cooling, and did not offer a significant resistance to water loss. Therefore, the OL did not require a mass balance for water. The mass balance for average water content (W , dry basis) in the food region was expressed using Eq. 4:

$$V_F c_s \frac{dW}{dt} = -\dot{R} S_\alpha \quad (\text{Eq. 4})$$

where, \dot{R} = rate for water loss. Eq. 4 states that the accumulation rate of water mass in potato cylinder ($V_F c_s dW/dt$) is equal to the evaporation rate ($N_{w,\alpha} = -\dot{R} S_\alpha$). The left-hand term in Eq. 4 was used to explain water loss from product in other simultaneous heat and mass transfer processes, such as drying and frying (Pakowski and Mujumdar, 2015; Ghaderi *et al.*, 2018). The term \dot{R} is modeled as a first order reaction dependent on the water concentration as recommended by Ghaderi *et al.* (2018) as shown in Eq. 5:

$$\dot{R} = k c_s W \quad (\text{Eq. 5})$$

The term \dot{R} should also be adjusted depending on product temperature. Arrhenius-based equations and logarithmic expressions of $p_{w,sat}$ have been used by other research groups to describe the temperature effect on evaporation rate during frying (Bansal *et al.*, 2014; Ghaderi *et al.*, 2018). In this case, the first order rate constant (k) was considered to depend on the saturation pressure of water ($p_{w,sat}$), a temperature function, using Eq. 6:

$$k = k_0 p_{w,sat} \quad (\text{Eq. 6})$$

where, k_0 = parameter adjusting the evaporation rate.

Energy balances

The energy balance in the OL was expressed in terms of global heat transfer coefficients evaluated at

oil side of α (OL-food) and β (OL-air) boundaries ($k_{hL,\alpha}$ and $k_{hL,\beta}$) as shown in Eq. 7:

$$V_L \rho_L C_{PL} \frac{dT_L}{dt} = k_{hL,\beta} (T_\beta - T_L) S_\beta + k_{hL,\alpha} (T_\alpha - T_L) S_\alpha \quad (\text{Eq. 7})$$

where, T_L , ρ_L , C_{PL} , and V_L = temperature, density, specific heat, and volume of the OL, respectively, T_α and T_β = temperatures at α and β boundaries, respectively, while S_β = contact surface between the OL and air regions. Eq. 7 expresses that accumulation rate of energy in the OL ($V_L \rho_L C_{PL} dT_L/dt$) results from the sum of energy fluxes crossing the OL-air ($q_{L,\beta} = k_{hL,\beta} (T_\beta - T_L) S_\beta$) and OL-food boundaries ($q_{L,\alpha} = k_{hL,\alpha} (T_\alpha - T_L) S_\alpha$), both evaluated at the OL side. Similarly, the energy balance in the potato cylinder was expressed using Eq. 8:

$$V_F \rho_F C_{PF} \frac{dT_F}{dt} = -k_{hF,\alpha} (T_F - T_\alpha) S_\alpha \quad (\text{Eq. 8})$$

where, T_F , ρ_F , C_{PF} , and V_F = temperature, density, specific heat, and volume of the potato specimen, respectively, while $k_{hF,\alpha}$ = heat transfer coefficient evaluated at the food side of α boundary (OL-food). Eq. 8 formulates that the rate of energy accumulation in the potato cylinder ($V_F \rho_F C_{PF} dT_F/dt$) equals the energy flux leaving the OL-food boundary ($-q_{F,\alpha} = k_{hF,\alpha} (T_\alpha - T_F) S_\alpha$), evaluated at the food side. Eqs. 7 and 8 resemble energy balances arising during the mathematical description of food drying (Pakowski and Mujumdar, 2015). The energy balance at the OL-air boundary was expressed using Eq. 9:

$$k_{hL,\beta} (T_\beta - T_L) S_\beta = h (T_{air} - T_\beta) S_\beta \quad (\text{Eq. 9})$$

Eq. (9) states that energy flux transferred from OL towards OL-air interface ($q_{L,\beta}$) equals the energy flux leaving this boundary towards the air ($q_{air,\beta} = h (T_{air} - T_\beta) S_\beta$). T_{air} = temperature of the surrounding air, and h = external (convective) heat transfer coefficient. On the other boundary, the energy flux transferred from the OL towards the OL-food interface ($q_{L,\alpha}$) splits in the energy flux transferred to the potato sample ($q_{F,\alpha}$) and the energy spent in water evaporation ($q_{w,\alpha} = \lambda N_{w,\alpha}$), as shown in Eq. 10:

$$k_{hL,\alpha} (T_\alpha - T_L) S_\alpha = k_{hF,\alpha} (T_F - T_\alpha) S_\alpha - \lambda \dot{R} S_\alpha \quad (\text{Eq. 10})$$

where, λ = latent heat of vaporisation of water. Energy balances given by Eqs. 9 and 10 imply that OL-food and OL-air boundaries do not accumulate energy.

Experimental validation

Debnath *et al.* (2009) reported the post-frying behaviour of potato cylinders obtained at different holding temperatures. Briefly, potato cylinders (1 cm diameter and 4 cm length) were fried at 180°C in palm olein for 5 min, and thereafter transferred to an air oven preheated at 100, 120, 140, 160 or 180°C. The potato cylinders were withdrawn from the oven after 5, 10, 15, 20, 30, 45, 60, 90, 120, 180, 240 or 300 s, and further analysed for their surface and inner (structure) oil contents as follows. The fried slices were immersed in hexane for 20 s to recover the oil adhered to their surfaces. After that, the extracted samples were oven-dried at 105°C for 24 h, and then analysed for their inner oil content by Soxhlet extraction with petroleum ether. Both surface and inner oil contents were expressed as mass of oil per mass of dry fat-free solids. The temperature of samples was also recorded by using a T-type thermocouple located at the geometric centre, and 0.5 mm below the surface. An additional experiment was conducted by holding the fried potato samples at room temperature (25°C). The oil contents and temperature data from those experiments were used in the present work, corresponding to the post-frying kinetics presented in Figure 3 (surface and penetrated surface oil contents) and Figure 4 (surface and centre temperatures).

Model solution

The post-frying heat and mass transfer differential-algebraic model formed by Eqs. 1 - 10 does not have an analytical solution, thus, it was numerically solved. Differential Eqs. 1, 4, 7, and 8 were integrated forward in time using a variable-order solver (ode15s) based on the numerical differentiation formulas with the Matlab® software (Matlab R2013a, MathWorks Inc., Natick, MA, USA). Eq. (9) was solved to evaluate the temperature at the OL-air interface (T_β) as shown in Eq. 11:

$$T_\beta = \frac{k_{hL,\beta} T_L + h T_{air}}{k_{hL,\beta} + h} \quad (\text{Eq. 11})$$

Unlike T_β , the temperature at the OL-food interface (T_α) cannot be explicitly solved from Eq. 10

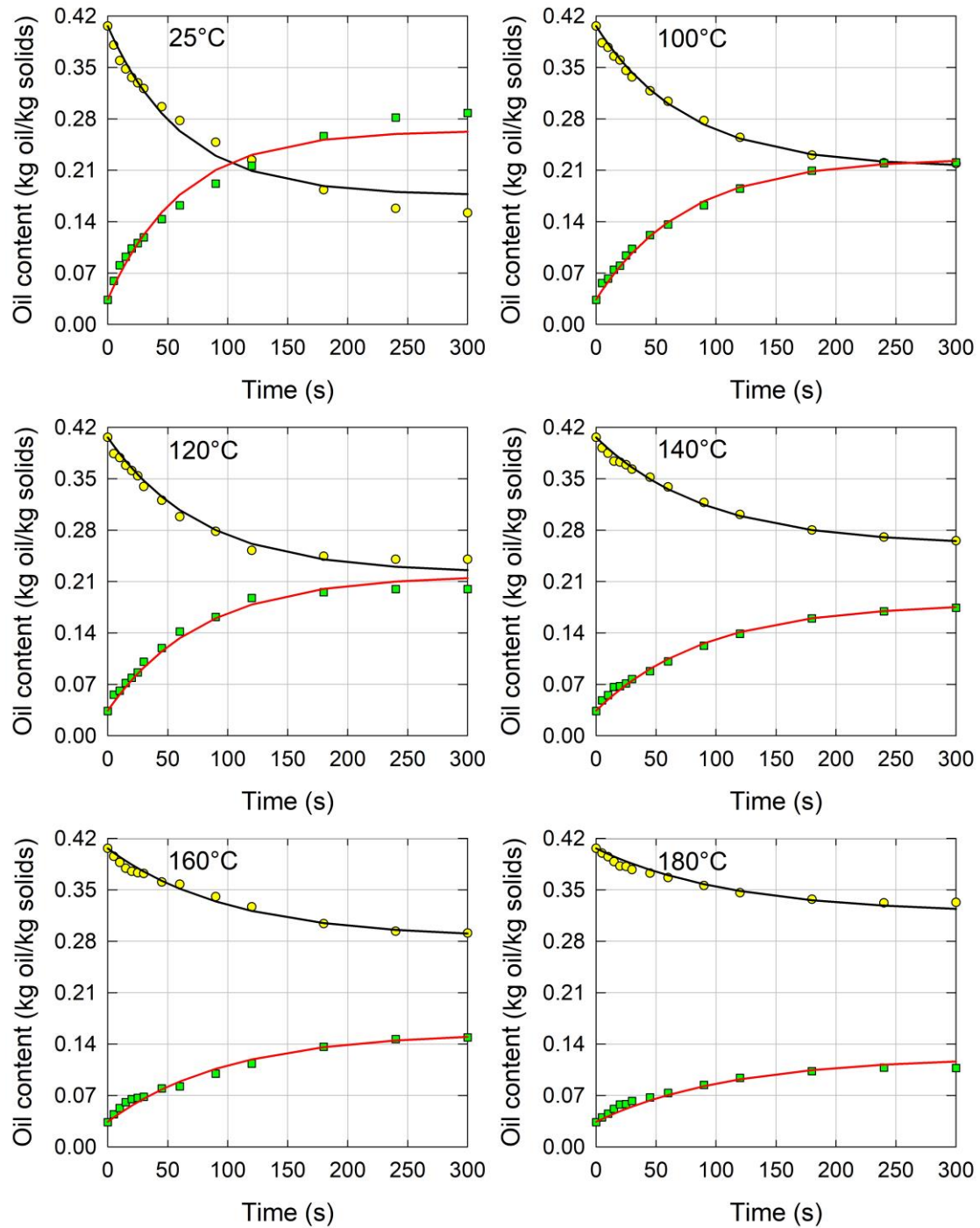


Figure 3. Experimental (dots) and predicted (lines) evolution of surface (circle symbols, black lines) and penetrated surface (square symbols, red lines) oil contents during post-frying of potato cylinders at different holding temperatures.

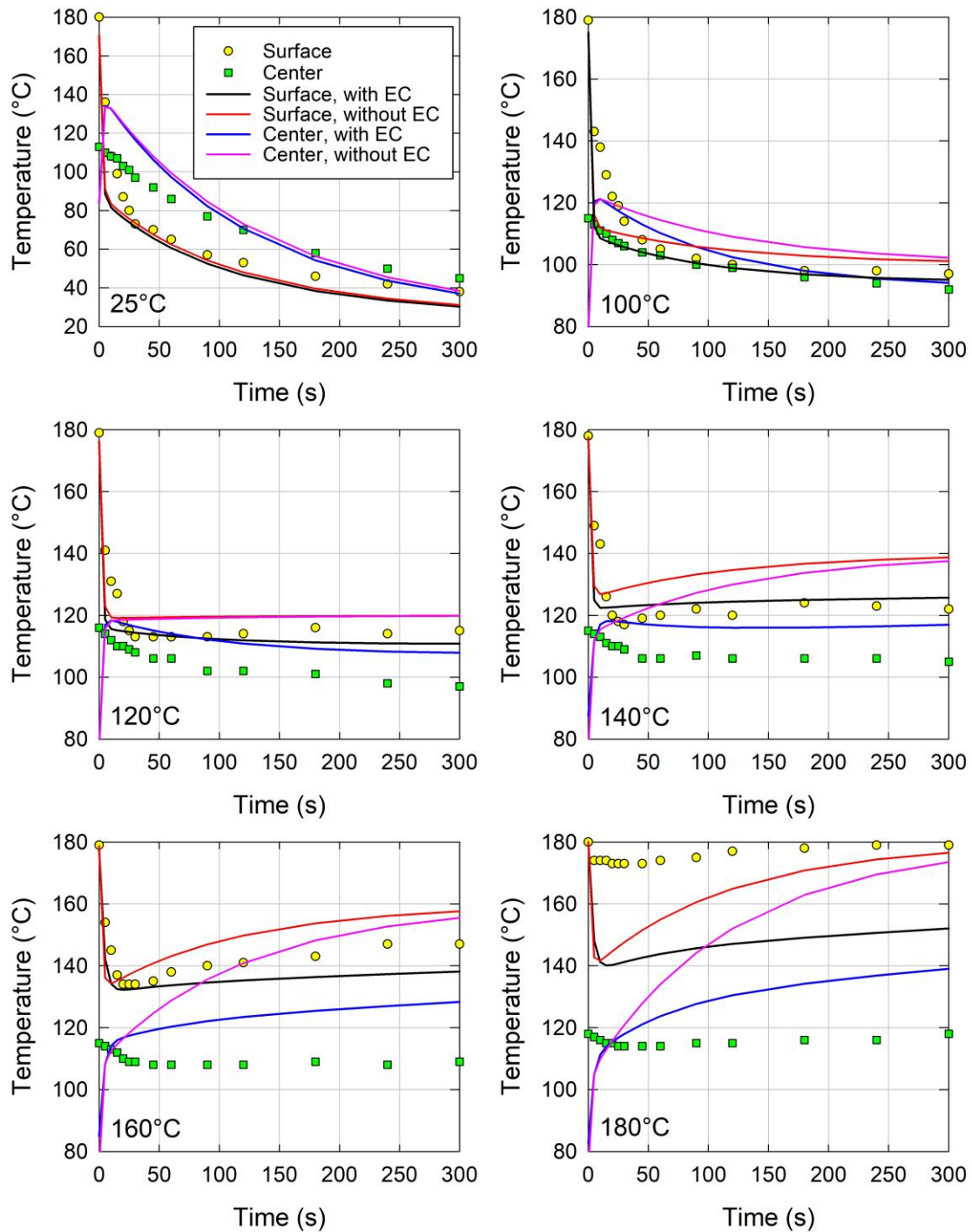


Figure 4. Experimental (dots) and predicted (lines) evolution of surface and centre temperatures during post-frying of potato cylinders at different holding temperatures. The model was solved with and without considering the effect of evaporative cooling (EC).

as λ and \dot{R} were also evaluated at this temperature. Therefore, Eq. 10 was numerically solved for T_α at each time-iteration with a combination of bisection, secant, and inverse quadratic interpolation methods,

implemented in the Matlab[®] routine `fzero`. Models to evaluate $p_{w,sat}$ (appearing in \dot{R}) and λ are given in Table 1.

Table 1. Summary of parameters used in the solution of post-frying oil absorption model.

Initial conditions for Eqs. (1), (2), (4), (7), and (8) (experimentally determined) (Debnath et al., 2009)
$Y_{init} = 0.034$ (g oil/g solids), $O_{init} = 0.406$ g oil/g solids, $W_{init} = 1.22$ g water/g solids; $T_{L,init} = 180^\circ\text{C}$; $T_{F,init} = 115^\circ\text{C}$
Composition of potato fat-free solids (g of component per g of fat-free solids, invariable during simulation) (ASHRAE, 2010)
$x_p = 0.0989$; $x_c = 0.7822$; $x_f = 0.0764$; $x_a = 0.0425$
Density (kg/m³) (ASHRAE, 2010)
$\rho_w = 997.18 + 0.0031439T - 0.0037574T^2$; $\rho_o = 925.59 - 0.41757T$; $\rho_p = 1329.9 - 0.5184T$; $\rho_c = 1599.1 - 0.31046T$; $\rho_f = 1311.5 - 0.36589T$; $\rho_a = 2423.8 - 0.28063T$; $\rho_F = \left(\frac{x_w}{\rho_w} + \frac{x_o}{\rho_o} + \frac{x_s}{\rho_s}\right)^{-1}$; $\rho_S = \left(\frac{x_p}{\rho_p} + \frac{x_c}{\rho_c} + \frac{x_f}{\rho_f} + \frac{x_a}{\rho_a}\right)^{-1}$
Specific heat (J/kg/°C) (ASHRAE, 2010)
$Cp_w = 4176.2 - 9.0864 \times 10^{-2}T + 5.4731 \times 10^{-3}T^2$; $Cp_o = 1984.2 + 1.4733T - 4.8008 \times 10^{-3}T^2$; $Cp_p = 2008.2 + 1.2089T - 1.3129 \times 10^{-3}T^2$; $Cp_c = 1548.8 + 1.9625T - 5.9399 \times 10^{-3}T^2$; $Cp_f = 1845.9 + 1.8306T - 4.6509 \times 10^{-3}T^2$; $Cp_a = 1092.6 + 1.8896T - 3.6817 \times 10^{-3}T^2$; $Cp_F = Cp_wX_w + Cp_oX_o + Cp_sX_s$; $Cp_S = Cp_px_p + Cp_cx_c + Cp_fx_f + Cp_ax_a$
Thermal conductivity (W/m/°C) (ASHRAE, 2010)
$\kappa_w = 0.57109 + 1.7625 \times 10^{-3}T - 6.7036 \times 10^{-6}T^2$; $\kappa_o = 0.18071 - 2.7604 \times 10^{-4}T - 1.7749 \times 10^{-7}T^2$; $\kappa_p = 0.17881 + 1.1958 \times 10^{-3}T - 2.7178 \times 10^{-6}T^2$; $\kappa_c = 0.20141 + 1.3874 \times 10^{-3}T - 4.3312 \times 10^{-6}T^2$; $\kappa_f = 0.18331 + 1.2497 \times 10^{-3}T - 3.1683 \times 10^{-6}T^2$; $\kappa_a = 0.32962 + 1.4011 \times 10^{-3}T - 2.9069 \times 10^{-6}T^2$; $\kappa_F = \kappa_wX_w + \kappa_oX_o + \kappa_sX_s$; $\kappa_S = \kappa_px_p + \kappa_cx_c + \kappa_fx_f + \kappa_ax_a$
Latent heat of vaporisation (λ, J/kg) and saturation pressure of water ($p_{w,sat}$, kPa) (Liley et al., 1997)
$\lambda = 2.8894 \times 10^6 \left(1 - \frac{T\theta}{647.13}\right)^{0.3199-0.212\left(\frac{T\theta}{647.13}\right)+0.25795\left(\frac{T\theta}{647.13}\right)^2}$; $p_{w,sat} = \frac{\exp\left(73.649 - \frac{7258.2}{T\theta} - 7.3037\ln(T\theta) + 4.1653 \times 10^{-6}(T\theta)^2\right)}{1000}$

The solution of the post-frying oil absorption model requires physical properties of both potato and OL, such as density, specific heat, and thermal conductivity. Potato properties were evaluated from composition rules based on weight fractions of protein (X_p), carbohydrates (X_c), fiber (X_f), ashes (X_a), oil (X_o), and water (X_w) (ASHRAE, 2010), where all components but water and oil were grouped into the fat-free solids ($X_s = X_p + X_c + X_f + X_a$). The mass fractions of oil (X_o), water (X_w), and fat-free solids (X_s) in potato cylinders relate to model variables Y and W in Eq. 12:

$$X_o = \frac{Y}{1+Y+W}; X_w = \frac{W}{1+Y+W}; X_s = \frac{1}{1+Y+W} \quad (\text{Eq. 12})$$

Composition equations were also applied to evaluate the density, specific heat, and thermal conductivity of fat-free solids. In this case, mass fractions relative to fat-free solids (x), which remain constant along process, were evaluated ($j = p, c, f, a$) as shown in Eq. 13:

$$x_j = \frac{X_{j,init}}{X_{p,init} + X_{c,init} + X_{f,init} + X_{a,init}} \quad (\text{Eq. 13})$$

The equations and parameters required to evaluate these properties are summarised in Table 1. A conduction mechanism was adopted for internal heat transfer coefficients. These quantities have the form (for $j = F, L$) as shown in Eqs. 14 and 15:

$$k_{hj,\alpha} = \frac{\kappa_j}{\delta_{j,\alpha}} = \frac{\kappa_j}{\phi_{j,\alpha}\Delta_j} \quad (\text{Eq. 14})$$

$$k_{hL,\beta} = \frac{\kappa_L}{\delta_{L,\beta}} = \frac{\kappa_L}{\phi_{L,\beta}\Delta_L} \quad (\text{Eq. 15})$$

where, δ = effective film thickness where the heat transfer occurs, Δ = characteristic length for conduction, and ϕ = geometrical factor defined by Eq. 16:

$$\phi = \frac{\sigma\Delta}{\lambda_1^2} \quad (\text{Eq. 16})$$

In Eq. 15, σ = specific surface, and λ_1 = first eigenvalue of the analytical variable separation solution for unsteady-state conduction equation under negligible convective resistance to heat transfer in a coordinate system able to represent the system geometry. Since potato was cut into cylinder, it had its radius (R) as the characteristic length for conduction ($\Delta_F = R$). On the other hand, the OL was a thin slab, where $\Delta_L = z$. The geometrical factors $\phi_{F,\alpha}$, $\phi_{L,\alpha}$, and $\phi_{L,\beta}$ can be evaluated as described by Martínez-Ramos *et al.* (2021), resulting in Eqs. 17 – 19:

$$\phi_{F,\alpha} = \frac{(S_\alpha/V_F)R}{\frac{\pi^2}{4\xi^2} + 2.4048^2} \quad (\text{Eq. 17})$$

$$\phi_{L,\alpha} = \frac{4(S_\alpha/V_L)z}{\pi^2} \quad (\text{Eq. 18})$$

$$\phi_{L,\beta} = \frac{4(S_\beta/V_L)z}{\pi^2} \quad (\text{Eq. 19})$$

where, ξ = length (l)-to-diameter ($2R$) ratio of the potato cylinders (Figure 1a). The effect of temperature on mass transfer coefficient in food was considered to follow an Arrhenius model as commonly seen in other transport properties (Marinos-Kouris and Maroulis, 2015), as shown in Eq. 20:

$$k_m = k_{m0} \exp\left(\frac{E}{R_g(T_F + 273.15)}\right) \quad (\text{Eq. 20})$$

where, k_{m0} = preexponential factor, E = activation energy, and R_g = universal gas constant.

The reduction in OL volume was calculated using Eq. 21:

$$V_L = \frac{m_o}{\rho_o} = \frac{m_{s,init}O}{\rho_o} = \frac{m_{F,init}X_{s,init}O}{\rho_o} \quad (\text{Eq. 21})$$

where, m = mass. For the cylindrical geometry, V_L = difference between volumes of oil-covered and uncovered potato cylinders (Figure 1a) as shown in Eq. 22:

$$V_L = \pi(R + z)^2(l + 2z) - \pi R^2l \quad (\text{Eq. 22})$$

The thickness of the OL (z) was determined by solving the expression resulting from combining Eqs. 21 and 22 into Eq. 23:

$$f(z) = \pi(R + z)^2(l + 2z) - \pi R^2l - \frac{m_{F,init}X_{s,init}O}{\rho_o} = 0 \quad (\text{Eq. 23})$$

Eq. 23 was solved in the same way as T_α at each time iteration. The parameters defining the rate of oil transfer within the potato sample (k_{m0} , E), the heat transfer between the OL and air (h), the rate for water loss (k_0), and the mass equilibrium for oil between the surface and food regions (K) were estimated by nonlinear regression as follows.

Debnath *et al.* (2009) reported the experimental evolution of four responses (surface and inner oil contents, and surface and centre temperature) at six holding temperatures. A much lower sampling time (≈ 10 s) was used to register temperature data; thus, interpolation was applied to obtain the thermal history of potato slices at the same times available for oil content (0, 5, 10, 15, 20, 30, 45, 60, 90, 120, 180, 240, and 300 s). Therefore, a total of 312 experimental data (78 data per variable) were available to estimate the parameters k_{m0} , E , h , k_0 , and K . The predicted surface temperature (T_β) was calculated from the heat balance at the OL-air boundary represented by Eq. 9 for its comparison with experimental data; however, the proposed model did not produce the centre temperature (T_{center}), thus, the procedure presented by Yang *et al.* (2021) was adapted for its estimation from centre and surface measurements. Briefly, a parabolic temperature profile was assumed between the centre and surface of potato cylinders along radial coordinate (the dominant heat and mass transfer direction) as shown in Eq. 24:

$$T(r, t) = T_{center}(t) + \left(T_{\beta}(t) - T_{center}(t) \right) \left(\frac{r}{R} \right)^2 \quad (\text{Eq. 24})$$

The volume-averaged temperature in the dominion (OL plus food) was obtained from $T(r, t)$ using Eq. 25:

$$T_{LF}(t) = \frac{\int_0^R T(r, t) r dr}{\int_0^R r dr} = \frac{1}{2} T_{center}(t) + \frac{1}{2} T_{\beta}(t) \quad (\text{Eq. 25})$$

Eq. 25 allows the estimation of T_{center} from T_{LF} and T_{β} . Here, the results for the temperatures of the OL and potato cylinders predicted with the post-frying model (T_L and T_F , respectively) was used to estimate T_{LF} using Eq. 26:

$$T_{LF}(t) = \frac{V_L T_L(t) + V_F T_F(t)}{V_L + V_F} \quad (\text{Eq. 26})$$

The following sum of squared errors (SSE) was minimised during the nonlinear regression procedure as shown in Eq. 27:

$$SSE = \sum_{k=1}^4 \sum_{j=1}^{78} \left(\frac{u_{exp,k,j} - u_{pred,k,j}}{u_{k,max}} \right)^2 \quad (\text{Eq. 27})$$

where, $u_1 = O$, $u_2 = Y$, $u_3 = T_{\beta}$, and $u_4 = T_{center}$, exp , $pred$, and max = experimental, predicted, and maximum value, respectively. The division by the maximum value was required to avoid the dominance of temperature residuals in the SSE due to their larger order of magnitude. As it occurs with other heat and mass transfer operations, mass equilibrium may exhibit a dependence on temperature and composition of the involved phases. However, as partition coefficients only provide an approximation of the real equilibrium behaviour within a limited range of the process variables, different coefficients could be needed when multiple experimental conditions are involved (Vargas-González *et al.*, 2021). Therefore, a separated value of K was estimated at each air temperature, as also performed by Debnath *et al.* (2009), resulting in ten estimated parameters (k_{m0} , E , h , k_0 , plus one K value for each of the six tested temperatures). The statistical significance of each estimated parameter was appraised with the 95% confidence intervals. Sequential regression was applied to systematically eliminate the non-significant parameters ($p > 0.05$) from the post-frying model. Finally, the fitness quality of the proposed

model for each treatment was evaluated as the mean relative deviation (MRD) using Eq. 28:

$$MRD = \frac{100}{13} \sum_{j=1}^{13} abs \left(\frac{u_{exp,j} - u_{pred,j}}{u_{exp,j}} \right) \quad (\text{Eq. 28})$$

where, u = each one of the fitted responses (O , Y , T_{β} , or T_{center}). Nonlinear regression was performed with the Matlab[®] routine `nlinfit` based on the Levenberg-Marquardt nonlinear least squares algorithm. All programs were run on a mainstream Lenovo[®] Legion Y720 laptop (Intel[®] Core™ i7-7700HQ processor, 16 GB DDR4 RAM, Nvidia[®] GeForce[®] GTX 1060 6GB graphic card).

Minimum oil penetration distance

An algorithm was developed to estimate the minimum oil penetration distance (d) during the post-frying period. The algorithm split the potato cylinder in two regions: (1) a dry zone where the oil was absorbed (V_1); and (2) a moist zone free from oil (V_2) (Figure 1b). The algorithm required Y , W , and T_F . The oil and water contents in the two regions were assigned as $Y_1 = Y$, $W_1 = 0$, $Y_2 = 0$, and $W_2 = W$. The volume of the moist region (V_2) was given in Eq. 29:

$$V_2 = \pi(R - d)^2(l - 2d) \quad (\text{Eq. 29})$$

The volume of the dry region (V_1) was evaluated as the difference between V_F and V_2 . The quantity $m_{s,init}$ was split into the regions 1 and 2 (for $k = 1, 2$) as shown in Eq. 30:

$$m_{sk} = \frac{V_k}{V_F} m_{s,init} \quad (\text{Eq. 30})$$

The weights of each potato region, and the oil and water they contained were calculated (for $k = 1, 2$) using Eq. 31:

$$m_{ok} = Y_k m_{s,init}; \quad m_{wk} = W_k m_{s,init}; \quad m_{Fk} = m_{ok} + m_{wk} + m_{sk} \quad (\text{Eq. 31})$$

Then, the density of each potato region was computed with (for $k = 1, 2$) Eq. 32:

$$\rho_{Fk}^* = \frac{m_{Fk}}{V_k} \quad (\text{Eq. 32})$$

The weight fractions of oil, water, and solids in each region were calculated (for $j = o, w, s$; $k = 1, 2$) with Eq. 33:

$$X_{jk} = \frac{m_{jk}}{m_{Fk}} \quad (\text{Eq. 33})$$

Weight fractions obtained with Eq. 33 were employed to estimate the density of each potato region (ρ_{Fk}) with composition equations presented in Table 1. Densities of regions 1 and 2 evaluated with compositional formulas should coincide with those evaluated with Eq. 32. Therefore, d must satisfy the objective function shown in Eq. 34:

$$f(d) = \text{abs}(\rho_{F1} - \rho_{F1}^*) + \text{abs}(\rho_{F2} - \rho_{F2}^*) = 0 \quad (\text{Eq. 34})$$

Results and discussion

The estimated heat and mass transfer parameters describing the post-frying oil absorption are summarised in Table 2. Mass transfer coefficient for oil in potato (k_m) was initially considered to follow an Arrhenius dependence on temperature; however, all regression attempts performed with several initial coefficient values produced non-significant estimates ($p > 0.05$) for Arrhenius model constants (refer to column “ k_m is a temperature function” in Table 2, where k_{m0} and E values appear in bold typeface). That is, no evidence of food temperature effect on k_m could be identified under the existing experimental conditions ($p > 0.05$).

Therefore, the temperature effect on k_m was discarded, and this parameter was further estimated as a unique constant value in a second regression procedure (refer to column “ k_m is a constant value” in Table 2), this time producing significant values for all parameters ($p < 0.05$). The obtained k_m value of 1.26×10^{-5} m/s can be compared to those reported by Debnath *et al.* (2009). These authors used the following oil transfer model (Eq. 35):

$$\frac{dY}{dt} = k_c(Y_e - Y) \quad (\text{Eq. 35})$$

where, Y_e = equilibrium oil content considered constant along the post-frying stage, and k_c = first-order rate constant. The comparison of Eqs. 1 and 35 revealed that k_c is equivalent to the ratio $k_m S_\alpha / V_F$. Debnath *et al.* (2009) reported separated k_c values for each holding temperature, ranging from 0.015 s^{-1} at 25°C to 0.009 s^{-1} at 180°C . The k_m estimation found in the present work produced a corresponding k_c value of 0.0064 s^{-1} , which was 57 to 93% lower than those given by Debnath *et al.* (2009). Eqs. 1 and 35 fundamentally differ in the way in which the driving potential for mass transfer is expressed ($Y_e - Y$ versus $Y_\alpha - Y$). In Eq. 3, O_α was set equal to O because of the assumption of negligible OL resistance to mass transfer. Under this assumption, Y_α instantaneously reaches its equilibrium value, but it decreases as

Table 2. Heat and mass transfer parameters describing the post-frying oil absorption of potato slices.

Parameter ^a	k_m is a temperature function ^b	k_m is a constant value ^b	Debnath <i>et al.</i> (2009) ^c
h	90 ± 20	89 ± 20	-
$k_0 \times 10^9$	4.9 ± 1.9	4.9 ± 1.9	-
K (25°C)	0.61 ± 0.22	0.66 ± 0.09	0.53 (25)
K (100°C)	0.93 ± 0.16	0.94 ± 0.13	0.99 (-5)
K (120°C)	1.01 ± 0.15	1.01 ± 0.14	1.22 (-17)
K (140°C)	1.45 ± 0.22	1.43 ± 0.21	1.56 (-8)
K (160°C)	1.86 ± 0.30	1.82 ± 0.29	1.93 (-6)
K (180°C)	2.68 ± 0.52	2.60 ± 0.48	3.07 (-15)
$k_{m0} \times 10^4$	1.3 ± 8.7	-	-
E	-7413 ± 22957	-	-
$k_m \times 10^5$	-	1.26 ± 0.24	-

(^a) Refer to nomenclature section to see the parameter units. Values in parentheses following K refer to the holding temperature. (^b) Mean \pm 95% confidence interval. Bold numbers indicate non-significant parameter estimates ($p > 0.05$). (^c) K values estimated as the ratio of surface (O)-to-structure (Y) oil contents at equilibrium. Values in parentheses represent the relative difference (%) with values obtained by using k_m as a constant value.

surface oil permeates the potato sample, while Y_e does not change. Therefore, the model by Debnath *et al.* (2009) uses the maximum driving force for mass transfer to estimate k_c in comparison with our model ($Y_e - Y > Y_\alpha - Y$), requiring k_c values lower than those of $k_m S_\alpha / V_F$ to predict identical oil absorption rates (dY/dt) when fitted to the same experimental data; nevertheless, this conclusion contradicts the observed results where $k_c > k_m S_\alpha / V_F$, requiring an additional explanation. Debnath *et al.* (2009) evaluated k_c as the slope of the plot of $\ln\left(\frac{Y - Y_e}{Y_{init} - Y_w}\right)$ versus t , as suggested by the analytical solution to Eq. 35. Therefore, observed differences in rate constants estimated in both studies could be attributed to different weighting caused by the response transformation, and the followed regression approach, where data for all responses and holding temperatures were simultaneously analysed, while Debnath *et al.* (2009) used a one-temperature-at-a-time approach.

Regarding the non-significant temperature effect found in the present work, a reliable estimation of mass transfer coefficients depends on experimental data associated with the initial transitory state (the dynamic period). Based on Figure 3, the transitory stage for mass transfer occurred during the first 120 s, where the surface and absorbed oil contents achieved at least the 70% of its final state. The experimental mean temperature of OL plus food (T_{LF}) was estimated using Eq. 26, and further time-averaged to obtain a representative value along this time frame. The time-averaged T_{LF} temperatures were 81, 108, 112, 116, 124, and 145°C at the holding temperatures of 25, 100, 120, 140, 160, and 180°C, respectively. Consequently, the covered temperature interval in terms of the averaged T_{LF} values (64°C) was much lower than that resulting from the holding temperatures (155°C), thus explaining why a unique k_m value was able to describe all post-frying kinetics.

An average oil diffusivity in food can be estimated if a diffusion formulation is adopted for mass transfer coefficient, as shown in Eq. 36:

$$k_m = \frac{D}{\delta_{F,\alpha}} = \frac{D}{\phi_{F,\alpha} \Delta_F} \tag{Eq. 36}$$

where, $\Delta_F = R$ and $\phi_{F,\alpha}$ was defined by Eq. 17. This approach produced an apparent oil diffusivity in potato of $2.7(\pm 0.5) \times 10^{-8}$ m²/s. The estimated oil diffusivity was comparable to that reported by Ateba and Mittal (1994) who determined a mean value of 2.87×10^{-8} m²/s during deep-fat frying of beef meatballs (159°C).

The use of higher holding temperatures increased the estimated distributions coefficients for oil (K , kg surface oil/kg absorbed oil), ranging from 0.66 at 25°C to 2.60 at 180°C ($p > 0.05$). These were very close to those estimated by Debnath *et al.* (2009) (Table 1), with minor discrepancies (in the order of 5 to 25%), which could have been due to differences in estimation methods and modelling assumptions as previously discussed for k_c .

The proposed post-frying model achieved a good description of all experimental responses (Figures 3 and 4) with MRD in the ranges of 0.9 - 4.8% (average 1.9%), 4.2 - 7.1% (average 5.9%), 4.0 - 16.9% (average 8.6%), and 8.4 - 16.0% (average 11.7%) for the surface oil content (O), inner oil content (Y), surface temperature (T_β), and centre temperature (T_{center}), respectively (Table 3). At a holding temperature of 25°C, the surface was cooler than the centre of product, but this trend inverted for increasing holding temperatures as the driving force for heat transfer between the surface and surrounding air was now decreased, and the surface began with a higher temperature at the start of the holding stage (Figure 4). At the end of the holding period (300 s), the experimental differences between surface and centre temperatures ($T_\beta - T_{center}$) were

Table 3. Fitness quality of post-frying model for investigated responses expressed as the mean relative deviation (MRD, %).

Response	Holding temperature (°C)						Average
	25	100	120	140	160	180	
O	4.8	1.1	2.2	0.9	1.3	1.3	1.9
Y	7.1	4.2	5.8	4.7	6.5	6.8	5.9
T_β	14.2	7.6	4.0	4.5	4.5	16.9	8.6
T_{center}	16.0	8.4	9.7	10.6	13.0	12.7	11.7

-7, 4, 18, 17, 38, and 61°C for the holding temperatures of 25, 100, 120, 140, 160, and 180°C, respectively, while the model predicted corresponding differences of -7, 1, 3, 5, 6, and 8°C. Since the precise placement of thermocouple at 0.5 mm below the potato surface may be challenging, our theory is that it was not truly registering the food temperature but also reflecting that of surrounding air, thus leading to a higher thermal gradient. This hypothesis was reinforced by observing the lack of the sharp drop of T_β to values below the holding temperature of 180°C at short times. In experiments conducted at holding temperatures of 120, 140 and 160°C, T_β decreased to 110, 120, and 140°C, respectively; yet, for holding at 180°C, it never did (Figure 4, continuous black line). Nevertheless, even if evaporative cooling effects were removed from the post-frying model ($k_0 = 0$), the sharp initial drop in T_β was still predicted during holding conducted at 180°C (Figure 2, dashed black line). As a result, the fairly constant history of T_β at 180°C could only be explained by the thermocouple recording the outside temperature. A comparison of plots in Figure 4 reveals that evaporative cooling contributed to a closer description of T_{center} (Figure 4, blue versus pink lines), as well as to an important reduction in water content of potato at temperatures of 100°C and above (Figure 5).

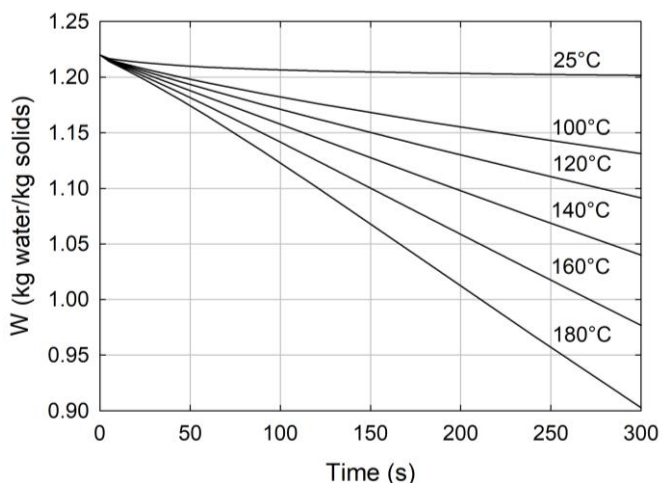


Figure 5. Predicted evolution of water content in food during post-frying of potato cylinders at different holding temperatures.

In this case, the post-frying model predicts a reduction from 1.22 kg water/kg solids to about 1.20 and 0.90 water/kg solids at the end of the monitoring period for the holding temperatures of 25 and 180°C,

respectively. If water content is expressed as the weight fraction of whole fried good (OL plus food), these values represent a change from 0.459 to 0.455 g water/g product at 25°C, and to 0.385 g water/g product at 180°C. A few selected studies have investigated the water loss occurring during the cooling stage of fried potato products. For example, Tarmizi and Niranjani (2013a) performed the frying of potato chips (3 - 4 min) and pre-fried frozen French fries (3.5 min) at 180°C. Oil-drainage was performed at the end of frying under vacuum (1.33 kPa) and atmospheric pressure (presumably at room temperature). The authors observed a significant reduction in moisture content during cooling period in vacuum drained fries (from about 0.38 to 0.02 g water/g solids for potato chips, and from 0.82 to 0.43 g water/g solids for French fries); however, no significant change in water content of potato fries was observed for atmospheric cooling. Bouchon and Pyle (2005a) formulated a post-frying model where the amount of water loss by evaporation was negligible; the experimental evidence presented by Tarmizi and Niranjani (2013a), as well as the currently simulated results, suggested that this hypothesis was correct, at least for cooling at room temperature. Nevertheless, an increased water loss at higher holding temperatures was expected, as these temperatures were just below or exceeded the common value used in ovens for moisture content analyses (105°C). The water evaporation at higher temperatures can also explain the lower oil absorption. According to Bouchon and Pyle (2005a; 2005b) and He *et al.* (2012), once the food is removed from oil, the water vapour in sample rapidly decreases because of a fast temperature reduction, thus increasing the pressure gradient for oil suction.

Based on the current procedure, the heat transfer coefficient (h) was about 89 W/m²/°C, which was in the range of those expected for forced convection during drying of food products with air (Marinos-Kouris and Maroulis, 2015); unfortunately, the experimental details (air velocity, airflow direction relative to product samples) allowing the calculation of this parameter with Nusselt correlations were unavailable, thus requiring its estimation from experimental data. Bouchon and Pyle (2005a) considered a linearised boundary condition, where convective and radiant effects are included in a single heat transfer coefficient, with an equivalent formulation as pure convective heat transfer. If

radiative heat transfer was accepted in the present work, then its effect would be already included in the estimated h value. As a result, radiation and convection mechanisms cannot solely explain the thermal history of food at temperatures above 100°C , thus making the formulation of evaporative cooling of utmost importance.

During frying, a dry crust develops at the food surface, thickness of which depends on frying time and temperature (Lioumbas and Karapantsios, 2012; van Koerten *et al.*, 2015). This crust retains most of the oil gained by food at the end of the post-frying cooling period (Bouchon *et al.*, 2001; 2003). The algorithm previously can be used to estimate the evolution of the minimum distance for oil penetration (d) by assuming the absorbed oil concentrates, in a layer immediately below the potato surface. In this case, the penetrated surface OL increased from an estimated length of $65\ \mu\text{m}$ immediately after frying to about 506 and $229\ \mu\text{m}$ at the end of the post-frying stage for the holding temperatures of 25 and 180°C , respectively (Figure 6a). On the other hand, the surface OL started at $486\ \mu\text{m}$ and decreased to between 211 and $394\ \mu\text{m}$ after 5 min (Figure 6b). The d value at 25°C showed a good agreement with previously published results, where post-frying stage was conducted at room temperature. For potato cylinders fried at 185°C for 3 min, the penetration distance of oil has been experimentally determined at

about $500\ \mu\text{m}$ (Bouchon *et al.*, 2001). The distance for oil penetration is very often associated to crust thickness (Bouchon *et al.*, 2003). Ziaifar *et al.* (2010) reported crust thicknesses of about 564 and $630\ \mu\text{m}$ in French fries ($8 \times 8 \times 60$ mm) cooked at 170 and 185°C for 360 s, respectively. Based on micrographs presented by Lioumbas and Karapantsios (2012), the average crust thickness (evaluated by image analysis) was between 469 and $533\ \mu\text{m}$ for potato sticks ($9.8 \times 9.8 \times 20$ mm) fried at 180°C for 200 and 400 s, respectively. A crust thickness of about $400\ \mu\text{m}$ is generally observed in potato for frying times around 2 min as highlighted by van Koerten *et al.* (2015). Yet, these authors reported a crust thickness of $950\ \mu\text{m}$ for potato cylinders (10 mm diameter and 50 mm length) fried for the same time at 180°C . This increase in thickness with frying temperature comes from the very definition of crust used by the authors (the evaporative region where just enough water is evaporated to create pores) unlike most of the existing literature, where crust is just the dry part of the fry (Miranda and Aguilera, 2006; Ziaifar *et al.*, 2010; Lioumbas and Karapantsios, 2012). In the present work, the minimum oil penetration distance was defined as an oil-saturated dry region, similarly as some crust definitions previously used, thus explaining the good agreement with crust thickness data.

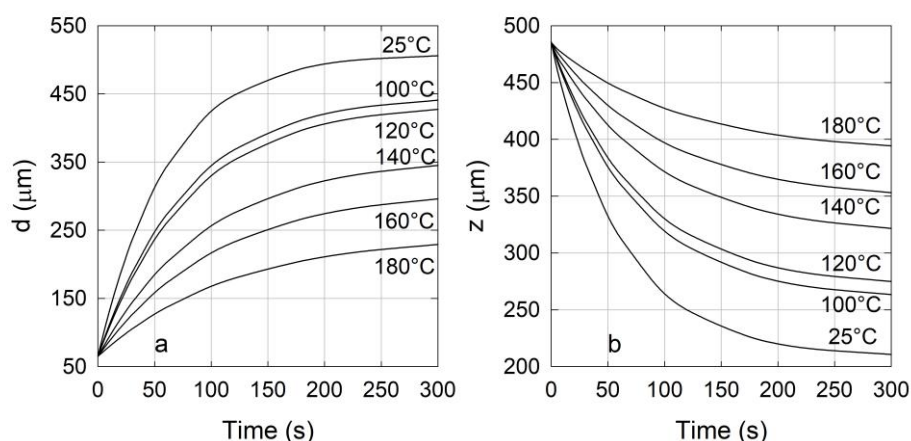


Figure 6. Predicted evolution of (a) minimum distance for oil penetration and (b) oil layer thickness in food during post-frying of potato cylinders at different holding temperatures.

Conclusion

The proposed model reproduced post-frying for both oil absorption and temperature behaviours of potato cylinders at different holding temperatures, with average deviations of 1.9 to 11.7%. While the

model provided average temperature values for the OL and the potato cylinder, the energy balance at OL-air boundary and the assumption of a parabolic temperature distribution allowed the estimation of the surface and centre temperatures for their comparison with experimentally collected values. As

demonstrated, the proposed model could be applied in the solution of inverse problems for the estimation of parameters related with convective heat transfer, oil penetration, water evaporation, and oil distribution. It was demonstrated that evaporative cooling became essential to achieve a precise description of the post-frying thermal history of potato cylinders for increasing holding temperatures. The minimum distance for oil penetration showed a good agreement with crust thickness values from literature; thus, the proposed algorithm could be potentially implemented in frying models as a mean to evaluate the growth of the crust region.

Acknowledgement

Jisel del Rosario Santiago acknowledges CONAHCYT for her doctoral scholarship (grant no.: 633571). Dr. Irving Israel Ruiz López acknowledges CONAHCYT for the financial support (grant no: CF19-194782) received in the completion of the present work.

References

- Al Faruq, A., Khatun, M. H. A., Azam, S. M. R., Sarker, M. S. H., Mahomud, M. S. and Jin, X. 2022. Recent advances in frying processes for plant-based food. *Food Chemistry Advances* 1: 100086.
- American Society of Heating, Refrigerating and Air-Conditioning Engineers (ASHRAE). 2010. 2010 ASHRAE Handbook - Refrigeration. United States: ASHRAE.
- Ateba, P. and Mittal, G. S. 1994. Modelling the deep-fat frying of beef meatballs. *International Journal of Food Science and Technology* 29: 429-440.
- Bansal, H. S., Takhar, P. S. and Maneerote, J. 2014. Modeling multiscale transport mechanisms, phase changes and thermomechanics during frying. *Food Research International* 62: 709-717.
- Bouchon, P. and Pyle, D. L. 2005a. Modelling oil absorption during post-frying cooling. I - Model development. *Foods and Bioproducts Processing* 83: 253-260.
- Bouchon, P. and Pyle, D. L. 2005b. Modelling oil absorption during post-frying cooling. II - Solution of the mathematical model, model testing and simulations. *Foods and Bioproducts Processing* 83: 261-272.
- Bouchon, P., Aguilera, J. M. and Pyle, D. L. 2003. Structure oil-absorption relationships during deep-fat frying. *Journal of Food Science* 68: 2711-2716.
- Bouchon, P., Hollins, P., Pearson, M., Pyle, D. L. and Tobin, M. J. 2001. Oil distribution in fried potatoes monitored by infrared microspectroscopy. *Journal of Food Science* 68: 2711-2716.
- Debnath, S., Rastogi, N. K., Krishna, G. and Lokesh, B. R. 2009. Oil partitioning between surface and structure of deep-fat fried potato slices: A kinetic study. *LWT - Food Science and Technology* 42: 1054-1058.
- Dehghannya, J. and Ngadi, M. 2021. Recent advances in microstructure characterization of fried foods - Different frying techniques and process modeling. *Trends in Food Science and Technology* 116: 786-801.
- Devi, S., Zhang, M., Ju, R. and Bhandari, B. 2020. Water loss and partitioning of the oil fraction of mushroom chips using ultrasound-assisted vacuum frying. *Food Bioscience* 38: 100753.
- Ghaderi, A., Dehghannya, J. and Ghanbarzadeh, B. 2018. Momentum, heat and mass transfer enhancement during deep-fat frying process of potato strips - Influence of convective oil temperature. *International Journal of Thermal Sciences* 134: 485-499.
- Gouyo, T., Goujot, D., Bohuon, P. and Courtois, F. 2021b. Multi-compartment model for heat and mass transfer during the frying of frozen pre-fried French fries. *Journal of Food Engineering* 305: 110587.
- Gouyo, T., Rondet, É., Mestres, C., Hofleitner, C. and Bohuon, P. 2021a. Microstructure analysis of crust during deep-fat or hot-air frying to understand French fry texture. *Journal of Food Engineering* 298: 110484.
- He, D.-B., Xu, F., Hua, T.-C. and Song, X.-Y. 2012. Oil absorption mechanism of fried food during cooling process. *Journal of Food Process Engineering* 36: 412-417.
- Khalilian, S., Mba, O. I. and Ngadi, M. O. 2021. Frying of eggplant. *Journal of Food Engineering* 293: 110358.
- Kim, T. and Moreira, R. G. 2013. De-oiling and pretreatment for high-quality potato chips.

- Journal of Food Process Engineering 36: 267-275.
- Kumar, V., Sharma, H. K., Singh, K., Kaushal, P. and Singh, R. P. 2017. Effect of pre-frying drying on mass transfer kinetics of taro slices during deep fat frying. *International Food Research Journal* 24: 1110-1116.
- Liberty, J. T., Dehghannya, J. and Ngadi, M. O. 2019. Effective strategies for reduction of oil content in deep-fat fried foods - A review. *Trends in Food Science and Technology* 92: 172-183.
- Liley, P. E., Thomson, G. H., Friend, D. G., Daubert, T. E. and Buck, E. 1997. Physical and chemical data. In Perry, R. H., Green, D. W. and Maloney, J. O (eds). *Chemical Engineers' Handbook*. United States: McGraw-Hill.
- Lioumbas, J. S. and Karapantsios, T. D. 2012. Evaporation front compared with crust thickness in potato deep-fat frying. *Journal of Food Science* 71: E17-E25.
- Marinos-Kouris, D. and Maroulis, Z. B. 2015. Transport properties in the drying of solids. In Mujumdar, A. S. (ed). *Handbook of Industrial Drying*. United States: CRC Press.
- Martínez-Ramos, T., Corona-Jiménez, E. and Ruiz-López, I. I. 2021. Analysis of ultrasound-assisted convective heating/cooling process - Development and application of a Nusselt equation. *Ultrasonics Sonochemistry* 74: 105575.
- Miranda, M. L. and Aguilera, J. M. 2006. Structure and texture properties of fried potato products. *Food Reviews International* 22: 173-201.
- Pakowski, Z. and Mujumdar, A. S. 2015. Basic process calculations and simulations in drying. In Mujumdar, A. S. (ed). *Handbook of Industrial Drying*. United States: CRC Press.
- Promraksa, A., Siripitana, C., Rakmak, N. and Chusri, N. 2020. Modeling of supercritical CO₂ extraction of palm oil and tocopherols based on volumetric axial dispersion. *The Journal of Supercritical Fluids* 166: 105021.
- Sosa-Morales, M. E., Solares-Alvarado, A. P., Aguilera-Bocanegra, S. P., Muñoz-Roa, J. F. and Cardoso-Ugarte, G. A. 2022. Reviewing the effects of vacuum frying on frying medium and fried food properties. *International Journal of Food Science and Technology* 57: 3278-3291.
- Tarmizi, A. H. A. and Niranjana, K. 2013a. Post-frying oil drainage from potato chips and French fries - A comparative study of atmospheric and vacuum drainage. *Food and Bioprocess Technology* 6: 489-497.
- Tarmizi, A. H. A. and Niranjana, K. 2013b. Combination of moderate vacuum frying with high vacuum drainage-relationship between process conditions and oil uptake. *Food and Bioprocess Technology* 6: 2600-2608.
- Thorpe, G. R. 2022. Modelling the rate of adsorption of carbon dioxide by wheat. *Journal of Stored Products Research* 97: 101970.
- Topete-Betancourt, A., Figueroa-Cárdenas, J. D. J., Morales-Sánchez, E., Arámbula-Villa, G. and Pérez-Robles, J. F. 2020. Evaluation of the mechanism of oil uptake and water loss during deep-fat frying of tortilla chips. *Revista Mexicana de Ingeniería Química* 19: 409-422.
- Torres-Ramón, E., García-Rodríguez, C. M., Estévez-Sánchez, K. H., Ruiz-López, I. I., Rodríguez-Jiménez, G. C., Romero de la Vega, G. and García-Alvarado, M. A. 2021. Optimization of a coconut oil extraction process with supercritical CO₂ considering economical and thermal variables. *The Journal of Supercritical Fluids* 170: 105160.
- Touffet, M., Trystam, G. and Vitrac, O. 2020. Revisiting the mechanisms of oil uptake during deep-frying. *Food and Bioprocess Technology* 123: 14-30.
- van Koerten, K. N., Schutyser, M. A. I., Somsen, D. and Boom, R. M. 2015. Crust morphology and crispness development during deep-fat frying of potato. *Food Research International* 78: 336-342.
- Vargas-González, S., Núñez-Gómez, K. S., López-Sánchez, E., Tejero-Andrade, J. M., Ruiz-López, I. I. and García-Alvarado, M. A. 2021. Thermodynamic and mathematical analysis of modified Luikov's equations for simultaneous heat and mass transfer. *International Communications in Heat and Mass Transfer* 120: 105003.
- Wanakamol, W. and Poonlarp, P. 2018. Effects of frying temperature, frying time and cycles on physicochemical properties of vacuum fried pineapple chips and shelf life prediction. *International Food Research Journal* 25: 2681-2688.
- Yang, S., Liu, T., Fu, N., Xiao, J. and Chen, X. D. 2021. Convective drying of highly shrinkable vegetables - New method on obtaining the

parameters of the reaction engineering approach (REA) framework. *Journal of Food Engineering* 305: 110613.

Zhou, X., Zhang, S., Tang, Z., Tang, J. and Takhar, P. S. 2022. Microwave frying and post-frying of French fries. *Food Research International* 159: 111663.

Ziaifar, A. M., Courtois, F. and Trystram, G. 2010. Porosity development and its effect on oil uptake during frying process. *Journal of Food Process Engineering* 33: 191-212.